Disappearance of Elliptic Flow: A New Probe for the Nuclear Equation of State

P. Danielewicz,[2] Roy A. Lacey,[1] P.-B. Gossiaux,[2,3] C. Pinkenburg,[1] P. Chung,[1] J. M. Alexander,[1] and R. L. McGrath[1]

[1]*Departments of Chemistry and Physics, State University of New York at Stony Brook, Stony Brook, New York 11794-3400*
[2]*National Superconducting Cyclotron Laboratory and the Department of Physics and Astronomy,*
Michigan State University, East Lansing, Michigan 48824-1321
[3]*SUBATECH, Ecole des Mines, F-44070 Nantes, France*

Using a relativistic hadron transport model, we investigate the utility of the elliptic flow excitation function as a probe for the stiffness of nuclear matter and for the onset of a possible quark-gluon-plasma phase transition at alternating-gradient synchrotron energies $1 \lesssim E_{\text{beam}} \lesssim 11A$ GeV. The excitation function shows a strong dependence on the nuclear equation of state, and exhibits characteristic signatures which could signal the onset of the transition.   [S0031-9007(98)07138-5]

PACS numbers: 25.75.Ld, 12.38.Mh, 24.10.Jv, 24.85.+p

The determination of the nuclear equation of state (EOS) has been, and continues to be, a major driving force for studies of nuclear matter at high-energy densities [1,2]. A prevailing notion is that such studies will not only provide crucial information about the EOS, but will afford unique information about novel nonperturbative aspects of quantum chromodynamics (QCD) [2,3]. The phase transitions for deconfinement and chiral symmetry restoration leading to quark-gluon plasma (QGP) formation constitute aspects which are of great current interest.

A key step toward the delineation of the EOS and the QGP phase transitions is the determination of experimental signatures which can serve as clean and sensitive probes. Many of the experimental signatures proposed over the last several years [4–6] have had only limited success, primarily because they have turned out to be sensitive not only to the EOS or the phase transition, but also to other poorly known physical effects.

Recent lattice QCD calculations (carried out at zero baryon density) point to a softening of the EOS near and above the energy region of the QGP phase transition, with the pressure rising with temperature more slowly than the energy density. This softening starts even for quark-antiquark densities quite comparable to those in the ground state of nuclear matter [7]. In the picture where changes in the properties of hadronic matter are associated with hadrons pushing out the nonperturbative vacuum, one expects a similar softening of the EOS even at relatively low temperatures when the baryon density increases significantly beyond its normal value ρ_0. Collisions of nuclei at alternating-gradient synchrotron (AGS) energies ($1 \lesssim E_{\text{beam}} \lesssim 11A$ GeV) are expected to produce equilibrated matter at densities up to $\rho \sim 8\rho_0$. Thus, it is of paramount importance to establish signatures for a softening of the EOS for such matter densities.

Pressure gradients provide the driving force for collective flow and the associated anisotropy of the transverse flow tensor. Consequently, flow measurements can provide useful probes for the pressure developed in nuclear collisions, and, hence, may provide insights into the EOS as well as QGP formation. The directed sideward flow signal at high energies is compromised by the fact that the flow angle essentially merges with the collision axis. In addition, this signal is known to exhibit strong dependencies on transport properties [8,9] which become increasingly uncertain with increasing beam energy. These dependencies are weaker for the transverse flow tensor (elliptic flow) which has already been shown to be quite sensitive to the pressure at maximum compression [10,11]. At AGS energies of $\sim(1-11)A$ GeV, the elliptic flow results from a strong competition between squeeze-out and in-plane flow. In the early stages of the collision as shown in Fig. 1(b), the spectator nucleons block the path of participant hadrons emitted toward the reaction plane; therefore the nuclear matter is initially squeezed out preferentially orthogonal to the reaction plane. This squeeze-out of matter leads to negative flow. In the later stages of the reaction as shown in Fig. 1(c), the geometry of the participant region (i.e., a larger surface area exposed in the direction of the reaction plane) favors in-plane preferential emission and hence positive elliptic flow. The magnitude and the sign of the elliptic flow depend on two factors: (i) the pressure built up in the compression stage compared to the energy density, and (ii) the passage time for removal of the shadowing due to the projectile and target spectators. Specifically, the characteristic time for the development of expansion perpendicular to the reaction plane is $\sim R/c_s$, where the speed of sound is $c_s = \sqrt{\partial p / \partial e}$, R is the nuclear radius, p is the pressure, and e is the energy density. The passage time is $\sim 2R/(\gamma_0 v_0)$, where v_0 is the center of mass spectator velocity. The squeeze-out contribution should then reflect the ratio $c_s/\gamma_0 v_0$ [8]. Measurements of the elliptic flow and of its excitation function should then provide a good probe of c_s and the EOS.

Theoretical efforts utilizing only hydrodynamical concepts have provided a wealth of qualitative insights on the nature of collective flow. However, these approaches often lead to serious overestimates of the quantitative strength of various dynamical effects [9,10,12]. In this
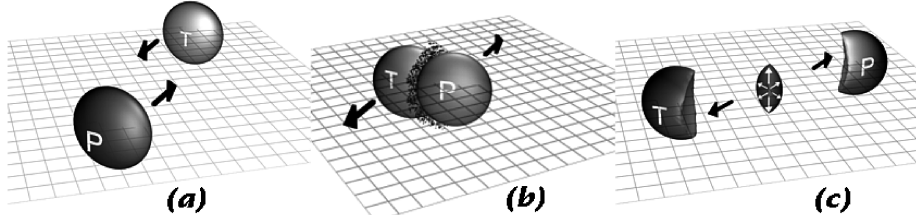
FIG. 1. Schematic illustration of the collision of two Au nuclei at relativistic energies. Time shots are shown for an instant before the collision (a), early in the collision (b), and late in the collision (c).

Letter, we investigate—by way of a relativistic transport model—the practical viability of elliptic flow as a probe for the EOS and the QGP in Au + Au collisions at AGS energies [$\sim(1-11)A$ GeV]. We show that (i) a distinct transition from negative to positive elliptic flow occurs at a beam energy, E_{tr}, which is strongly dependent on the parameters of the EOS, and (ii) that a phase transition to the QGP would provide a characteristic and detectable signature in the elliptic flow excitation function.

Calculations have been performed with a preliminary version of our new relativistic transport model [13]. An ultimate goal for this new effort is to have a model which is not only applicable at finite baryon densities and in nonequilibrium situations, but can reproduce the thermodynamic properties of nuclear matter obtained in lattice QCD calculations. The phenomenological relativistic Landau theory of quasiparticles [14] serves as a basis for the model. For the purpose of this Letter, which is concerned only with energies of $\sim(1-11)A$ GeV, we choose nucleons, pions, and Δ and N^* resonances for the hadronic degrees of freedom. Particle energies are evaluated by specifying the energy density (in any frame) as a functional of the particle phase-space distributions. The fields are chosen here solely to act on baryons as these particles offer the best chance to observe any emission anisotropy that is of a dynamic origin. Since the vector and scalar fields can be momentum dependent with no exclusive dependence on the vector or scalar densities, there is no particular benefit for a separate consideration of such fields (unless, of course, the spin dynamics were considered).

For convenience, we choose a parametrization for the fields that can easily be identified as either vector or scalar [15]. Thus, in the case of the fields without momentum dependence in their nonrelativistic reduction, we use a baryon energy density of the form

$$e = \sum_X \frac{g_X}{(2\pi)^3} \int d\mathbf{p}\, f_X(\mathbf{p}) \sqrt{p^2 + m_X^2(\rho_s)}$$
$$+ \int_0^{\rho_s} d\rho_s'\, U(\rho_s') - \rho_s U(\rho_s), \qquad (1)$$

where the summation is over all baryons, $m_X(\rho_s) = m_X + U(\rho_s)$, and $\rho_s = \sum_X \frac{g_X}{(2\pi)^3} \int d\mathbf{p} \times [m_X(\rho_s)/\sqrt{p^2 + m_X^2(\rho_s)}] f_X(\mathbf{p})$. This gives baryon single-particle energies

$$\epsilon_X(p, \rho_s) = \sqrt{p^2 + m_X^2(\rho_s)}. \qquad (2)$$

We take

$$U(\xi) = \frac{-a\xi + b\xi^\nu}{1 + (\xi/2.5)^{\nu-1}}, \qquad (3)$$

where $\xi = \rho_s/\rho_0$, $\rho_0 = 0.16$ fm^{-3}, and a, b, and ν are adjusted to the ground-state nuclear-matter properties: $a = 187.24$ MeV, $b = 102.62$ MeV, and $\nu = 1.5354$ for a soft equation of state ($K = 210$ MeV), and $a = 115.08$ MeV, $b = 48.25$ MeV, and $\nu = 2.5427$ for a stiff equation of state ($K = 380$ MeV). It is important to point out here that the denominator in (3) prevents supraluminous behavior at high densities. A steeper increase of energy with density for the stiff EOS (see inset of Fig. 3, shown below) leads to higher pressures and sound velocities for that equation.

In the case of mean fields dependent on momentum in their nonrelativistic reduction, we parametrize the energy density in the local frame where $\mathbf{J} = \sum_X \frac{g_X}{(2\pi)^3} \int d\mathbf{p}\, f_X(\mathbf{p}) \frac{\partial \epsilon_X}{\partial \mathbf{p}} = 0$, with

$$e = \sum_X \frac{g_X}{(2\pi)^3} \int d\mathbf{p}\, f_X(\mathbf{p}) \left(m_X + \int_0^p dp'\, v_X^*(p', \rho) \right)$$
$$+ \int_0^\rho d\rho'\, U(\rho'), \qquad (4)$$

and U is of the form expressed by Eq. (4) with $\xi = \rho/\rho_0$ and $\rho = \sum_X \frac{g_X}{(2\pi)^3} \int d\mathbf{p}\, f_X(\mathbf{p})$. Here the local particle velocity v_X^* is of the form

$$v_X^*(p, \xi) = \frac{p}{\sqrt{p^2 + m_X^2/(1 + c\frac{m_N}{m_X}\frac{\xi}{(1+\lambda p^2/m_X^2)^2})^2}}. \qquad (5)$$

This yields single-particle energies

$$\epsilon_X(p, \rho) = m_X + \int_0^p dp'\, v_X^*$$
$$+ \rho\left\langle \int_0^p dp'\, \frac{\partial v}{\partial \rho} \right\rangle + U(\rho),$$

which in a nonrelativistic reduction is similar to the energies in the nonrelativistic transport models proposed by Bertsch et al. [1,16]. Adjustment of the parameters to the properties of nuclear matter and to the nucleon-nucleus potential gives $a = 185.47$ MeV, $b = 36.29$ MeV, $\nu = 1.5391$, $c = 0.838\,89$, and $\lambda = 1.0890$ for a soft equation of state ($K = 210$ MeV), and $a = 123.62$ MeV, $b = 14.65$ MeV, $\nu = 2.8906$, $c = 0.835\,78$, and $\lambda = 1.0739$ for a stiff equation ($K = 380$ MeV). The effective mass at normal density and Fermi momentum is $m_N^* = p_F/(\partial \epsilon_N/\partial p) = 0.65 m_N$ for both sets.

The equations of motion in the mean field have been integrated utilizing a relativistic Hamiltonian for the computational lattice. In any simulation, it is important to satisfy detailed balance conditions for elementary collision processes close to equilibrium. It is difficult to satisfy

this condition for processes involving more than two particles in the final state [17]. Consequently, we adopt a compromise which results in a different treatment of the high-energy and low-energy collision processes. For the low-energy processes ($\sqrt{s} - m_1 - m_2 < 1.7$ GeV), we force at most two particles in any state, and a strict detailed balance is followed. This is in direct contrast to the high-energy processes for which the inverse processes are considered to be less likely. The high-energy production processes are parametrized using available experimental data on net cross sections, pion multiplicities, hadron rapidity, and transverse-momentum distributions (e.g., [18]); these processes are simulated using the concept of transverse-momentum phase space with a leading particle effect. The procedure is similar to that of Ref. [19]. When possible, the diffractive production is favored over the central. The low-energy processes are treated in a relatively standard manner [17]. The model, so constructed, successfully reproduces pion and proton rapidity distributions as well as transverse-momentum distributions within the beam-energy range of interest.

A necessary prerequisite for using elliptic flow as a probe for the EOS and the QGP is that a chosen measure of this flow can accurately determine both its magnitude and sign. To measure the elliptic azimuthal asymmetry of the particle distributions at midrapidity, we use the Fourier coefficient $\langle \cos 2\phi \rangle$, where ϕ represents the azimuthal angle of an emitted baryon ($|y_{\mathrm{cm}}| < 0.3 y_0$) relative to the reaction plane. In the absence of elliptic flow, this coefficient is zero. For in-plane elliptic flow (i.e., positive) the Fourier coefficient $\langle \cos 2\phi \rangle > 0$ and for out-of-plane flow (i.e., negative) $\langle \cos 2\phi \rangle < 0$. For small values of the ratio $c_s / \gamma_0 v_0$, the squeeze-out (or negative) contribution should decrease approximately linearly with this ratio.

An important characteristic of the elliptic flow is the change from negative values at low energies ($\sim 0.2 A$ GeV) to positive values at high beam energies ($\sim 20 A$ GeV). This behavior is clearly exhibited in Fig. 2(a) where we show elliptic flow excitation functions for calculations which assume a stiff EOS (filled diamonds) and a soft EOS (filled circles). For comparison we also show results from calculations without a mean field. All of the results shown in Fig. 2(a) are calculated for impact parameters of $b = 4-6$ fm. Figure 2(a) shows an essentially logarithmic dependence of the elliptic flow on beam energy over the range $0.5 \lesssim E_{\mathrm{beam}} \lesssim 10 A$ GeV. This trend is the expected qualitative result indicating that the squeeze-out contribution to the elliptic flow decreases with increasing beam energy. Figure 2(a) also shows that the slope of the excitation function, as well as the beam energy E_{tr}, for transition from negative to positive elliptic flow, depends strongly on the stiffness of the EOS. We believe that these results not only provide a new and significant probe for the EOS, but also raise the expectation that any change in the stiffness of the EOS with energy will be manifested as a change in the slope of the excitation function.

Experience from the low-energy domain ($E_{\mathrm{beam}} \lesssim 1 A$ GeV) has shown that the momentum dependence of the mean field is an important factor for the determination of the EOS from flow measurements. Nucleon-nucleus scattering data and nuclear-matter calculations clearly indicate the presence of this momentum dependence; here, it plays a role in generating flow before the matter equilibrates. *A priori,* there could be two separate effects due to the momentum dependence: (i) It may pass for an enhanced stiffness of the EOS, and/or (ii) it may lead to a loss of sensitivity to the stiffness of the EOS. The second effect could eliminate the possibility of observing a change in the stiffness with increasing beam energy.

In Fig. 2(b), we show elliptic flow excitation functions obtained from calculations that include momentum-dependent fields. The general trends of these excitation functions are similar to those shown in Fig. 2(a). However, one can clearly see that the net effect of the momentum dependence is to enhance the squeeze-out. Of greater significance is the fact that the sensitivity of the elliptic flow to the stiffness of the EOS remains practically unchanged when this momentum dependence is included. The difference in the transition energy E_{tr} is $\sim 2 A$ GeV, between the soft and stiff EOS whether or not one includes momentum-dependent forces (see Fig. 2). A cursory examination of Fig. 2 also shows that measurements of elliptic flow should clearly discriminate between models with a realistic EOS and the cascade models for which $E_{\mathrm{tr}} \lesssim 0.6 A$ GeV. The latter result corroborates an earlier finding on the second-order flow [20].
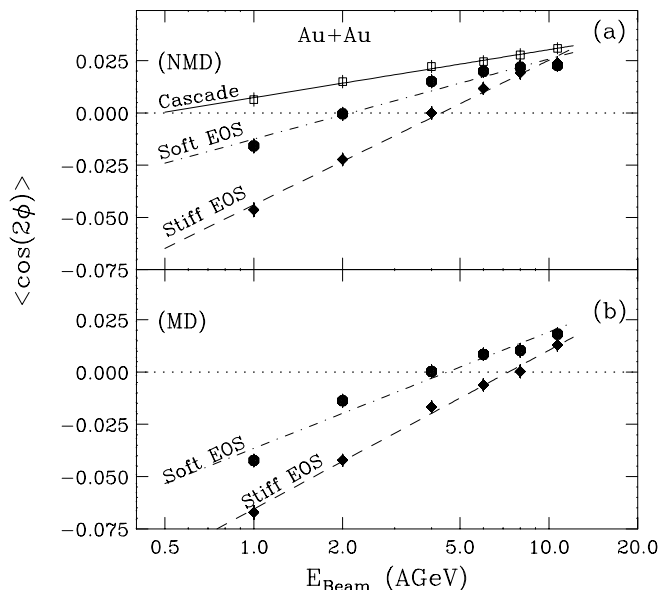

FIG. 2. Calculated elliptic flow excitation functions for Au + Au reactions. Panels (a) and (b) show, respectively, the functions obtained without (NMD) and with (MD) the momentum-dependent forces. The filled circles, filled diamonds, and open squares indicate, respectively, results obtained using a soft EOS, a stiff EOS, and by neglecting the mean field. The straight lines show logarithmic fits.
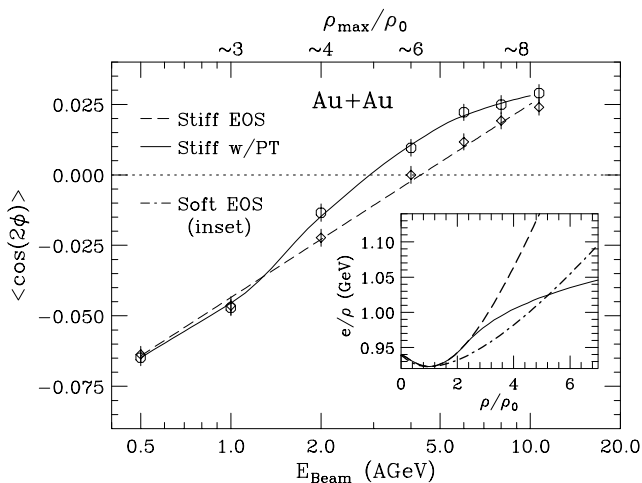
FIG. 3.   Calculated elliptic flow excitation functions for Au + Au. The open diamonds represent results obtained with a stiff EOS. The open circles represent results obtained with a stiff EOS and with a second-order phase transition (see text). The solid and dashed lines are drawn to guide the eye. Numbers at the top of the figure indicate rough magnitude of local baryon densities reached in reactions at different beam energies. The inset shows energy per baryon vs baryon density in the calculations, at $T = 0$, for a stiff EOS (dashed line), a stiff EOS with a second-order phase transition (solid), and a soft EOS (dash-dotted).

In order to search for an elliptic flow signature that can signal the onset of a phase transition to the QGP, we have carried out calculations assuming an EOS with a weak second-order phase transition, obtained by setting $U = $ const in (1)–(3), for $\xi \geq 2.3$. The energy per baryon for this EOS (solid line) is compared to that for the stiff EOS (dashed) in the inset of Fig. 3. A first-order phase transition with a stronger drop in the energy per baryon (in the same general density range) is obtained in the extrapolation of the lattice QCD results [13]. The elliptic flow excitation functions calculated using a stiff EOS with a phase transition (open circles) and a stiff EOS without the phase transition (diamonds) are compared in Fig. 3. Both functions have been obtained with no consideration of momentum dependence in the mean field. For low beam energies ($\lesssim 1A$ GeV), the flow excitation functions are essentially identical because the two EOS are either identical or not very different at the densities and temperatures that are reached. For $2 \lesssim E_{\text{beam}} \lesssim 9A$ GeV the excitation function shows larger in-plane elliptic flow from the calculation which includes the phase transition, indicating that a softening of the EOS has occurred for this beam-energy range. This deviation is in direct contrast to the essentially logarithmic beam-energy dependence obtained (for the same energy range) from the calculations which assume a stiff EOS without the transition. This difference in the predicted excitation functions could very well serve as an important hint as to whether or not the conditions necessary for the phase transition to the QGP are created in this energy range.

In summary, we have used a relativistic hadron transport model to investigate the viability of elliptic flow as a probe for the compressibility of nuclear matter and the onset of a possible QGP phase transition in the energy range $(1-11)A$ GeV. The flow excitation functions obtained from our calculations indicate that a distinct transition from out-of-plane elliptic flow to in-plane elliptic flow occurs at a beam energy, E_{tr}, which is strongly dependent on the incompressibility constant for nuclear matter. Additional calculations, which take account of a possible phase transition, show characteristic trends in the excitation functions for flow, which could signal the onset of a QGP phase transition. These new results suggest that an experimental analysis of elliptic flow from reaction data at AGS energies can provide invaluable constraints for the EOS and possibly for formation of the QGP.

[1] G. F. Bertsch and S. Das Gupta, Phys. Rep. **160**, 189 (1988).
[2] E. V. Shuryak, Phys. Rep. **61**, 71 (1980).
[3] D. J. Gross et al., Rev. Mod. Phys. **53**, 43 (1981).
[4] P. J. Siemens and J. I. Kapusta, Phys. Rev. Lett. **43**, 1486 (1979).
[5] T. Matsui and H. Satz, Phys. Lett. B **334**, 416 (1986).
[6] C. B. Dover, Nucl. Phys. **A590**, 333c (1995).
[7] E. Laermann, Nucl. Phys. **A610**, 1c (1996).
[8] P. Danielewicz, Phys. Rev. C **51**, 716 (1995).
[9] P. Danielewicz, in *Proceedings of the Workshop on Physics of Intermediate and High Energy Heavy Ion Reactions, Kraków, 1987,* edited by M. Kutschera (World Scientific, Singapore, 1988), p. 141.
[10] J.-Y. Ollitrault, Phys. Rev. D **46**, 229 (1992).
[11] H. Sorge, Phys. Rev. Lett. **78**, 2309 (1997).
[12] D. H. Rischke et al., Heavy Ion Phys. **1**, 309 (1995).
[13] P.-B. Gossiaux, in Proceedings of the 14th Winter Workshop on Nuclear Dynamics, Snowbird, 1998 (to be published).
[14] G. Baym and S. A. Chin, Nucl. Phys. **A262**, 527 (1976).
[15] Q. Pan and P. Danielewicz, Phys. Rev. Lett. **70**, 2062 (1993); **70**, 3523 (1993).
[16] L. P. Csernai et al., Phys. Rev. C **46**, 736 (1992). For completeness, it should be noted that for matter without local reflection symmetry in momentum space, there is a correction term in Eq. (7) from $\mathbf{J} = 0$ that we ignore here; it is interesting that this term is never mentioned in connection with nonrelativistic calculations.
[17] P. Danielewicz and G. F. Bertsch, Nucl. Phys. **A533**, 712 (1991).
[18] D. Horn, Phys. Rep. **4**, 1 (1972); H. Grässler et al., Nucl. Phys. **B132**, 1 (1978); Yu. A. Budagov et al., Fiz. Elem. Chastits At. Yadra **11**, 687 (1980).
[19] Y. Pang et al., Brookhaven National Laboratory Report No. BNL-49626, 1993.
[20] M. B. Tsang et al., Phys. Rev. C **53**, 1959 (1996).